Published in final edited form as:
Nat Cell Biol. 2012 August ; 14(8): 818–828. doi:10.1038/ncb2532.

Centralspindlin and α-catenin regulate Rho signalling at the epithelial zonula adherens

Aparna Ratheesh[#1,6], **Guillermo A. Gomez**[#1], **Rashmi Priya**[1], **Suzie Verma**[1], **Eva M. Kovacs**[1], **Kai Jiang**[2], **Nicholas H. Brown**[3], **Anna Akhmanova**[2], **Samantha J. Stehbens**[1,4], and **Alpha S. Yap**[1,6]

[1]Division of Molecular Cell Biology, Institute for Molecular Bioscience, The University of Queensland, St. Lucia, Brisbane, Queensland, Australia 4072 [2]Cell Biology, Faculty of Science, Utrecht University, Padualaan 8, 3584 CH, Utrecht, The Netherlands [3]Gurdon Institute and Department of Physiology, Development and Neuroscience, Cambridge University, Tennis Court Rd, Cambridge CB2 1QN, UK

[#] These authors contributed equally to this work.

Summary

The biological impact of Rho depends critically on the precise subcellular localization of its active, GTP-loaded form. The spatio-temporal balance between molecules that promote nucleotide exchange or GTP hydrolysis can potentially determine the sites of Rho signalling. But how these activities may be coordinated is poorly understood. We now report a molecular pathway that achieves exactly this coordination at the epithelial zonula adherens. We identify an extramitotic activity of the centralspindlin complex, better understood as a cytokinetic regulator, which localises to the zonula adherens during interphase by interacting with the cadherin-associated protein, α-catenin. Centralspindlin recruits the Rho GEF, Ect2, to the zonula adherens to activate Rho and support junctional integrity through myosin IIA. Centralspindlin also inhibits the junctional localisation of p190RhoGAP B, which can inactivate Rho. Thus, a conserved molecular ensemble that governs Rho activation during cytokinesis is utilized in interphase cells to control the Rho GTPase cycle at the zonula adherens.

Keywords

E-cadherin; junctions; Rho; centralspindlin; Ect2; α-catenin

Introduction

Rho family GTPases are fundamental regulators of cell behaviour, that are active and able to engage with downstream effectors when present in their GTP-loaded state[1]. The nucleotide status of these small GTPases is determined by the action of guanosine nucleotide exchange factors (GEFs) that catalyse GTP-loading, and GTPase-activating proteins (GAPs) that stimulate Rho proteins to convert bound GTP to GDP[2].

The biological impact of Rho also depends on the precise subcellular site where Rho-GTP is expressed[3]. This influences the effector molecules that are available to interact with active

[6]Correspondence to: Aparna Ratheesh: aparnaratheesh@gmail.com Alpha Yap: a.yap@uq.edu.au.
[4]Current address: Department of Cell and Tissue Biology, University of California, San Francisco, San Francisco, CA

Europe PMC Funders Author Manuscripts

Rho and hence the cellular processes it can regulate. Indeed, studies that immunolocalised endogenous Rho or used biosensors to identify Rho-GTP have identified distinctive distribution patterns for Rho signalling that depend consistently on the biological context of the cells[4-7]. This is exemplified by cytokinesis, where Rho accumulates in a sharply-defined zone at the contractile furrow and regulates actomyosin-based processes necessary for cell division[6,8,9]. Importantly, the precise spatio-temporal control of this Rho zone is necessary for orderly cell division[3,8].

During interphase epithelial cells display prominent Rho localisation at their cell-cell junctions[5,10]. Rho signalling is necessary for cell-cell integrity[11,12] and this is likely to substantially reflect local regulation of the actomyosin cytoskeleton. Potential Rho effectors at junctions include nonmuscle myosin II[13] and regulators of actin dynamics, such as formins[14]. For example, we recently reported that myosin IIA localises to junctions in a Rho/ROCK-dependent fashion, where it serves as a cortical organizer that promotes E-cadherin clustering and accumulation in the zonula adherens (ZA)[13]. Both loss- and gain-of Rho function perturb junctional integrity[11,12], indicating that stringent expression of Rho signalling at junctions plays a key role in cell-cell cohesion. However, the molecular mechanism that concentrates Rho-GTP at junctions is poorly understood. Formally, coordinate regulation of the GEF and GAP limbs of its GTPase cycle provides an attractive way to control the spatial expression of the Rho-GTP signal[3,12]. However, for this to occur there must be mechanisms that spatially coordinate the localisation of relevant Rho GEFs and GAPs to cadherin junctions. We now report that the centralspindlin complex, a key regulator of Rho signalling during cytokinesis[9], carries out an extramitotic function to regulate GEF/GAP balance, and preserve junctional integrity, at the epithelial zonula adherens.

Results

The zonula adherens is a microtubule-dependent Rho zone

We began by comparing the subcellular distribution of RhoA and E-cadherin in confluent, interphase MCF7 mammary epithelial monolayers. E-cadherin distributed extensively throughout the lateral surfaces of the cells, forming both a prominent apical ring denoting the zonula adherens[15] and puncta that lie throughout the lateral surface below the zonula adherens (Fig 1a,b)[13,16]. Indirect immunofluorescence microscopy in TCA-fixed specimens[5] also revealed conspicuous endogenous RhoA staining at cell-cell contacts (Fig 1a). Three-dimensional reconstruction of confocal stacks demonstrated further that, while Rho was distributed quite extensively throughout the lateral cell surfaces, it concentrated in the region of the zonula adherens (Fig 1a,b). This suggested that the zonula adherens might represent a Rho zone in interphase epithelial cells, akin to the contractile ring of the cytokinetic furrow[3,17].

C3-transferase (C3T) significantly reduced Rho staining at junctions (Fig 1c,d), indicating that GTP-loading of Rho was necessary for its steady-state concentration at the zonula adherens. This further implied that a significant proportion of junctional Rho was likely to be in the GTP-loaded state. We tested this using a FRET-based Rho biosensor where energy transfer occurs when the RhoA module is GTP-loaded[4]. Like endogenous Rho, the Rho biosensor distributed in the cytoplasm and concentrated at cell-cell junctions (Fig 1e, CFP channel). However, greater energy transfer was detected in the junctional pool than in the cytoplasmic pool (Fig 1f) and this was reduced by C3T (Fig 1e,g). Thus, cadherin-based cell-cell junctions are prominent sites of Rho signalling in interphase epithelial cells. Mechanisms must then exist to ensure that Rho is activated, and maintained in an active state, at those junctions.

Previously we demonstrated that cadherin junctions and their associated cytoskeleton are influenced by dynamic microtubules[18]. In particular, nocodazole, used at a concentration (100 nM) that blocks microtubule plus-end dynamics without depolymerising the lattice[19,20], prevented the junctional accumulation of myosin IIA, but not that of myosin IIB (Fig 1h, Fig S1a). As myosin IIA, but not myosin IIB[13], requires Rho signalling to concentrate at the zonula adherens[13,21], this suggested that dynamic microtubule plus-ends might regulate junctional Rho.

Indeed, Rho at the zonula adherens was substantially reduced by 100 nM nocodazole (Fig 1i,j). Furthermore, nocodazole reduced junctional Rho FRET to levels comparable to C3T treatment (Fig 1k,l). Junctional Rho (Fig 1m, Fig S1b) and myosin IIA (Fig S1c) were also substantially reduced when dynamic microtubule plus ends were independently perturbed by shRNA knockdown of End-binding (EB) proteins 1 and 3 (Fig S1b), which bind to, and regulate protein-protein interactions at, dynamic plus-ends[22,23]. Thus the zonula adherens appeared to be a microtubule-dependent Rho zone.

Ect2 activates Rho signalling at the zonula adherens

Pursuing this observation, we then examined the cellular localisation of candidate Rho GEFs known to be influenced by microtubules. Strikingly, we found clear junctional localisation for Ect2 (Fig 2a,b), but not GEF-H1 (not shown), in interphase MCF7 cells. Ect2 is a Rho GEF that is best understood to operate during mitosis where it localizes to the contractile furrow (Fig S2a) and activates Rho[9,24,25]. With some exceptions[26], it is commonly reported to be a nuclear protein during interphase[24], though these studies were generally performed in isolated cells that did not make adhesive contacts with one another. We found that while nuclear Ect2 was detectable in confluent MCF7 cells, it also clearly localized at cell-cell contacts (Fig 2a), an observation that we confirmed in Caco-2 and MDCK cells[26] (Fig S2b). Furthermore, within cell-cell contacts Ect2 selectively localised to the zonula adherens (Fig 2a,b), characteristically at its apical margin. Little Ect2 staining associated with the cadherin clusters found elsewhere on the lateral cell surface (Fig 2b). The specificity of this immunofluorescence pattern was confirmed by Ect2 RNAi, which abolished junctional and nuclear staining (Fig S2c,e), and further corroborated by transiently-expressed GFP-Ect2, which also localised to cell-cell contacts (Fig S2d). Of note, junctional Ect2 staining was significantly reduced by both low-dose nocodazole (Fig 2c,d) and EB1/3 shRNA (Fig 2e), exactly the maneuvers that inhibited Rho signalling at junctions. Thus, Ect2 was an attractive candidate to mediate microtubule-dependent Rho signalling at the zonula adherens.

To test this notion, we infected MCF7 cells with lentiviral shRNA directed against the 3′ UTR of the human Ect2 gene, which reduced cellular Ect2 expression by ~90% (Fig 2f). Indeed, junctional Rho, notably its characteristic concentration at the zonula adherens, was substantially reduced in Ect2 knockdown cells compared with cells infected with a control virus (Fig 2g,h). Similar changes were seen when Ect2 was depleted by siRNA (Fig S2e,f). Junctional Rho was restored in Ect2 shRNA cells by expression of an RNAi-resistant transgene (Fig 2g,h), indicating that the changes in Rho were attributable to manipulation of Ect2 itself. Finally, use of the Rho FRET biosensor confirmed that Rho-GTP was reduced at the zonula adherens in Ect2 shRNA cells compared with control-infected cells and restored by expression of RNAi-resistant Ect2 (Fig 2i,j). Together, these findings identify Ect2 as a major activator of Rho signalling at the zonula adherens.

Ect2 signalling regulates zonula adherens integrity and apical junction tension

The zonula adherens is a specialized adhesive junction that supports epithelial cohesion and apical contractility[27]. Its integrity requires Rho signalling to the actomyosin cytoskeleton[13,28].

We found that Ect2 knockdown disrupted the zonula adherens. In contrast to control cells, Ect2-deficient cells failed to concentrate E-cadherin in the apical ring pattern of the zonula adherens (Fig 3a,b, Fig S2g), although strands and clusters of cadherin persisted at the lateral contacts (Fig 3a). In contrast, tight junctions identified by ZO-1 staining remained present in Ect2-knockdown cells (Fig S3a, b), indicating a relatively selective effect on the zonula adherens. As neither total nor surface levels of E-cadherin were altered by Ect2 knockdown (Fig S3c), we postulated that the defect arose from failure of surface cadherin to be concentrated and retained in an apical junctional structure. To test this, we expressed E-cadherin-EGFP in cadherin knock-down cells[29] and measured fluorescence recovery after photobleaching the apical region. Ect2 knockdown and C3T both decreased the immobile fraction and the half-time of recovery (Fig 3c, Suppl Table 1), indicating more rapid turnover of apical E-cadherin. This implies that Ect2-Rho signaling stabilizes E-cadherin mobility at the apical junctional zone.

To better understand how Ect2 stabilizes cadherin, we then examined its effects on the junctional actomyosin cytoskeleton. Surprisingly, F-actin staining in the apical ring at the zonula adherens was not substantively affected by Ect2 knockdown or by inhibiting Rho directly with C3T (Fig S3d,e). Instead, Ect2 knockdown depleted myosin IIA, but not myosin IIB, from apical junctions (Fig 3d,e). Myosin IIA depletion perturbs the zonula adherens in a very similar manner to Ect2 knockdown[13] and, indeed, myosin IIA shRNA increased apical E-cadherin-EGFP mobility (Fig 3c, Suppl table 1), similarly to Ect2 knockdown or C3T. These findings thus suggested that Ect2 supports zonula adherens integrity through myosin IIA. If so, we predicted that junctional integrity might be restored in Ect2 shRNA cells if the amount of myosin IIA at the junctions could be increased. Indeed, zonula adherens integrity was restored to Ect2 knockdown cells by exogenous expression of GFP-myosin IIA (Fig 3f,g), thus reinforcing the notion that myosin IIA is a downstream effector of Ect2 at the zonula adherens. As Rho is necessary for myosin IIA to concentrate at the zonula adherens[13] and acute treatment with C3T displaced myosin IIA, but not Ect2, from junctions (Fig S3f,g), Ect2 presumably recruits myosin IIA indirectly by activating Rho.

The coordination of actomyosin contractility with cadherin adhesion can also generate tension at the zonula adherens[30], a process implicated in coordinating cell-cell movements and patterning within epithelia[31,32]. To test whether Ect2 signaling influences junctional tension, we used a femtosecond laser as a nanoscissor to cut junctions and measured the instantaneous recoil of the junction at its vertices as an index of junctional tension[32]. Junctional tension was reduced by Ect2 knockdown and also by inhibiting Rho or depleting myosin IIA (Fig 3 h,i, S3h). Thus the Ect2-Rho-myosin IIA pathway supports epithelial junctional tension.

Overall, these findings identify a novel, extra-mitotic role for Ect2 to support cell-cell interactions between interphase epithelial cells. We propose that selective localisation of Ect2 to the zonula adherens promotes local Rho signalling. This ultimately signals to recruit and activate myosin IIA[13,21], which stabilizes apical cadherin to preserve the integrity of the zonula adherens and support junctional tension.

The centralspindlin complex mediates microtubule-dependent junctional localisation of Ect2

To better understand how dynamic microtubules influence junctional Ect2 we measured fluorescence recovery after photobleaching junctional GFP-Ect2 expressed in Ect2 knock-down cells (Fig S4a). Nocodazole reduced the immobile fraction, without significantly affecting $T_{1/2}$, suggesting that dynamic microtubules might influence cortical binding of Ect2 at junctions. In parallel, we screened Ect2 immunoprecipitates by mass spectrometry to identify potential junctional binding partners (not shown). Amongst these we found MKLP1, a component of the centralspindlin complex. Centralspindlin is a heterotetramer, consisting of two copies each of MKLP1, a member of the kinesin superfamily, and MgcRacGAP, a GAP that can directly bind to Ect2[33]. During cytokinesis centralspindlin localizes Ect2 to activate Rho at the contractile furrow[9,25] and we therefore wondered if it might play a similar role at the zonula adherens during interphase.

Indeed, immunostaining for endogenous MgcRacGAP and MKLP1 revealed that both proteins localised to microtubule-dense interphase cell-cell junctions in confluent MCF7 monolayers, as well as in nuclei, as has been previously reported in isolated cells[34](Fig 4a, Fig S4b). Of note, like Ect2 (Fig 2a) both centralspindlin components selectively concentrated with E-cadherin in the apical zonula adherens (shown for MgcRacGAP in Fig 4a). RNAi of either protein abolished this staining pattern (Fig S4c,d) and junctional localisation was further confirmed by transiently expressed GFP-tagged MgcRacGAP and MKLP1 (Fig S4e). These findings thus identified centralspindlin as a novel junctional constituent in interphase epithelial cells.

We then used RNAi (Fig S4c) to assess if centralspindlin affected junctional Ect2 and Rho signalling. siRNAs against either MgcRacGAP or MKLP1 substantially reduced junctional Ect2 staining (Fig 4b,c) without affecting total cellular Ect2 (Fig 4d), but Ect2 RNAi did not affect junctional MgcRacGAP or MLKP1 (Fig S4f). This suggested that centralspindlin functions upstream to control the junctional localisation of Ect2. Similarly, both components of the centralspindlin complex are needed to localise Ect2 to the contractile furrow during cytokinesis[9,25].

Consistent with their impact on junctional Ect2, junctional Rho was reduced in either MKLP1 or MgcRacGAP knockdown cells (Fig 4e,f) and GTP.Rho was reduced by MgcRacGAP depletion (Fig 4g). Further, myosin IIA was selectively lost from junctions in either MKLP1 or MgcRacGAP knockdown cells (Fig 4h, S4g). Overall, these data implicate centralspindlin in localising Ect2 to the ZA, with consequent signalling through Rho to myosin IIA. Supporting a central role for centralspindlin in junctional signalling, the integrity of the zonula adherens was also perturbed in both MKLP1 and MgcRacGAP knockdown cells (Fig 4i, S4g) in a manner similar to that seen when Ect2, Rho or myosin IIA were inhibited.

Interestingly, junctional localization of centralspindlin was reduced by 100 nM nocodazole (Fig 4j,k), making it an attractive candidate to mediate the microtubule-dependent localisation of Ect2 to junctions. Indeed, the nocodazole-sensitivity of junctional Ect2 was abolished by MgcRacGAP RNAi (Fig 4l). Thus, whereas in control cells junctional Ect2 was reduced by nocodazole and recovered upon washout of the drug, MgcRacGAP knockdown cells showed a lower baseline level of Ect2 that was not affected by addition or removal of nocodazole. This suggests that centralspindlin contributes to the microtubule-dependence of junctional Ect2.

α-catenin localizes Ect2 to the zonula adherens through centralspindlin

Binding to centralspindlin alone did not readily explain the specific localization of Ect2 to the zonula adherens. Thus we were interested to also identify α-catenin in our Ect2 interaction screen (not shown), a finding that was confirmed by reciprocal co-immunoprecipitation analysis (Fig 5a). E-cadherin also co-precipitated with Ect2 (Fig 5a) and both α-catenin and Ect2 were identified in E-cadherin immune complexes (Fig 5a) suggesting that junctional Ect2 might exist in a complex with E-cadherin and α-catenin. Consistent with this, Ect2, α-catenin and E-cadherin co-localised at the zonula adherens (Fig 5b, Fig S5a), but with little colocalization between Ect2 and α-catenin below the zonula adherens (Fig S5a).

To test its impact on junctional Ect2, we depleted α-catenin by siRNA (Fig S5b) and examined cells 24 hrs after transfection, when junctional α-catenin was significantly diminished, but cell-cell contacts remained intact (Fig 5b). Ect2 was significantly reduced at junctions of α-catenin knockdown cells (Fig 5b,c). Indeed, Ect2 was often undetectable at junctions that retained significant residual α-catenin (Fig 5b), suggesting that its junctional localisation was quite sensitive to α-catenin. Consistent with this, the biochemical association of E-cadherin with Ect2 was also reduced by α-catenin knockdown (Fig 5d). Thus α-catenin also contributes to the junctional localization of Ect2.

We then asked whether centralspindlin was involved in the interaction between α-catenin and Ect2. Both E-cadherin and α-catenin co-immunoprecipitated with MgcRacGAP (Fig 6a), suggesting that centralspindlin could associate with the cadherin-catenin complex. Further, MgcRacGAP knockdown significantly reduced the amount of Ect2 that coimmunoprecipitated with α-catenin (Fig 6b), without affecting the interaction between E-cadherin and α-catenin (Fig 6c). These data imply that centralspindlin serves as an intermediate to localise Ect2 to α-catenin at the zonula adherens. Consistent with this, α-catenin knockdown substantially reduced both junctional MgcRacGAP and MKLP1 (Fig 6d,e) but MgcRacGAP knockdown had only minor impact on junctional α-catenin (Fig 6f,g) probably due to loss of the mature zonula adherens. Further, nocodazole reduced the interaction between MgcRacGAP and α-catenin (Fig 6h), suggesting that dynamic microtubules might regulate this interaction to support junctional Ect2.

To better characterize the molecular basis of these interactions, we expressed GFP-tagged α-catenin mutants in HEK293 cells (Fig 6i, S5d). Both endogenous Ect2 and MgcRacGAP consistently co-precipitated with FL-α-catenin and with N-terminal fragments of α-catenin (1-290, 1-507), but not with a C-terminal fragment (507-906). Thus the N-terminus of α-catenin appears to mediate its association with centralspindlin and Ect2. We therefore conclude that α-catenin serves as a cortical anchor for centralspindlin at the zonula adherens, to thereby support the Ect2-Rho signalling pathway.

This model further predicted that α-catenin would influence junctional Rho signalling. Indeed, both junctional Rho (Fig 5e,f) and Rho-GTP (Fig 5 g,h) were reduced in α-catenin knockdown cells. Consistent with our evidence that myosin IIA is a downstream effector of junctional Ect2-Rho signalling, we also found that myosin IIA, but not myosin IIB, was reduced at junctions of α-catenin knockdown cells (Fig S5c). Thus α-catenin regulates Rho-based signalling at the zonula adherens.

Centralspindlin inhibits the junctional recruitment of p190B RhoGAP

Finally, we asked whether centralspindlin might also influence junctional Rho by regulating its inactivation. The spatial expression of a Rho-GTP signal is influenced by the localised action of RhoGAPs as well as by RhoGEFs[3,35]. In particular, p190RhoGAP has been implicated in cadherin junctions[36,37] and in regulating Rho signalling at the cytokinetic

furrow[35,38,39]. Given our evidence for conserved pathways that regulate Rho during cytokinesis and at junctions, we examined the impact of dynamic microtubules on the subcellular localisation of p190 RhoGAP during interphase in epithelial monolayers.

Two members of this protein family exist in mammals[40,41] and both p190A RhoGAP and p190B RhoGAP were detected in MCF7 cells by immunoblotting (Fig 7f). In control MCF7 monolayers both forms of p190 RhoGAP also showed predominantly cytoplasmic staining with little apparent at the junctions (Fig 7a). Strikingly, however, junctional p190B RhoGAP became distinctly evident after inhibition of microtubule plus-end dynamics with nocodazole (100 nM), a three-fold increase being confirmed by linescan analysis (Fig 7b,c). In contrast, p190A RhoGAP remained cytoplasmic in nocodazole-treated cells (Fig 7b). This suggested that dynamic microtubules might specifically inhibit the junctional accumulation of p190B RhoGAP, but not of p190A RhoGAP.

Since dynamic microtubules support the junctional localisation of the centralspindlin complex, we then asked whether centralspindlin might play a role in regulating the junctional accumulation of p190B RhoGAP. Indeed, junctional p190B RhoGAP staining was significantly increased in both MgcRacGAP and MLKP1 knockdown cells but not in cells transfected with control siRNAs or where Ect2 was depleted (Fig 7d,e). Together, these data suggested that the microtubule-dependent localisation of centralspindlin at the zonula adherens might also promote junctional Rho-GTP by blocking recruitment of p190B RhoGAP, as well as through local activation of Rho by Ect2.

To test this notion, we then asked if the increased junctional p190B RhoGAP contributed to the reduced Rho found at junctions in nocodazole-treated cells. We predicted that if this were so, then reducing p190B RhoGAP should modulate the impact of nocodazole on junctional Rho. Accordingly, we used siRNA to selectively deplete p190B RhoGAP but not p190A RhoGAP (Fig 7f). Nocodazole reduced junctional Rho and Rho-GTP in cells transfected with control siRNAs (Fig 7g,h), exactly as it did in untransfected cells (Fig 1j). Strikingly, however, nocodazole did not reduce junctional Rho (Fig 7g, S6a) or Rho-GTP (Fig 7h) to the same level in p190B RhoGAP knockdown cells as it did in control cells. This implies that p190B RhoGAP contributed to the inhibition of Rho by nocodazole.

p190B RhoGAP contains a GTP-Rac binding domain that regulates its cortical recruitment[40]. As cell-cell contacts can be sites of Rac signalling[7], we therefore wondered whether p190B RhoGAP was recruited to junctions in response to Rac. Indeed, the junctional accumulation of p190B RhoGAP induced by nocodazole was reduced by expression of a dominant-negative Rac mutant (N17; Fig 7i) or treatment with the Rac inhibitor, NSC 23766 (Fig S6b). Further, a p190B RhoGAP mutant lacking the Rac-interaction domain[40] did not localize to junctions in nocodazole-treated cells (Fig S6c). Thus, the nocodazole-induced recruitment of p190B RhoGAP appears to require Rac signalling. Potentially, then, the microtubule-centralspindlin pathway may block p190B RhoGAP recruitment by inhibiting junctional Rac. Indeed, using a Raichu-Rac FRET biosensor we found that junctional GTP-Rac was increased both by nocodazole and MgcRacGAP knockdown (Fig 7j, S6d). Together, these suggest that centralspindlin may inhibit junctional p190B RhoGAP recruitment by reducing junctional Rac signaling.

Discussion

In sum, our findings identify the epithelial zonula adherens as a Rho zone that is an interphase equivalent of the Rho zone of the cytokinetic furrow[8,9]. Like the cytokinetic furrow, the Rho zone of the zonula adherens serves to concentrate actomyosin activity, acting through myosin IIA to maintain the integrity of the junction itself. Remarkably, Rho

signalling at the zonula adherens is controlled by many of the same molecules that regulate Rho at the cytokinetic furrow. The key role is played by the centralspindlin complex, which supports the junctional Rho zone by regulating both the activation and inactivation limbs of the GTPase cycle: it activates Rho by recruiting the Rho GEF Ect2 and prevents Rho inhibition by blocking the junctional recruitment of p190B RhoGAP (Suppl. Fig S7). Recruitment of Ect2 is likely to reflect its known direct interaction with MgcRacGAP[9,25] while we postulate that centralspindlin blocks p190B RhoGAP recruitment by directly or indirectly inhibiting junctional Rac signalling[40]. Of note, both Ect2 and p190 RhoGAP have also been implicated in Rho regulation at the cytokinetic furrow[9,25,35,39], although other GAPs, including MgcRacGAP itself[3] may also contribute. This indicates that the Rho zone of the zonula adherens reflects the action during interphase of a conserved molecular ensemble that can translate coordinated regulation of the Rho GTPase cycle into spatial expression of an active Rho signal at the junction.

From this perspective, a key issue is how centralspindlin is localised to the zonula adherens. Here we identify a novel function for α-catenin to support the cortical binding of centralspindlin, and thereby Ect2, at the zonula adherens. Thus, although we first identified α-catenin as an Ect2 binding protein, we subsequently found that it binds to centralspindlin as well as to Ect2 and E-cadherin, suggesting that they may form a molecular complex. Further α-catenin depletion displaced centralspindlin from junctions and uncoupled Ect2 from the cadherin, while depleting MgcRacGAP uncoupled Ect2 from α-catenin. Together, these observations argue that α-catenin interacts with centralspindlin to thereby localize Ect2 to the zonula adherens.

This finding carries the important implication that α–catenin can influence cadherin biology by regulating Rho signalling at the zonula adherens. Consistent with this, α–catenin knockdown reduced both Rho signalling and the cortical recruitment of myosin IIA. Of note, also, these effects were observed under conditions of incomplete α–catenin depletion, when the zonula adherens was perturbed but cells remained in contact with one another. At later times after siRNA transfection cells detached from one another, a more extreme phenotype that may reflect the other pathways by which α–catenin can affect cadherin function[42,43]. Thus Rho regulation may be a relatively sensitive effect of α–catenin on cadherin biology. Interestingly, Drosophila α–catenin has been reported to associate with Rho itself[10], suggesting that multiple mechanisms may exist to allow α-catenin to regulate Rho signaling at cadherin junctions.

It was striking that both centralspindlin and Ect2 selectively localised to the zonula adherens, which, although the cortical site for a major pool of endogenous Rho, was not the only site for Rho staining at the lateral cortex of cell-cell contacts. Moreover, Ect2 and the centralspindlin complex appeared to selectively support zonula adherens integrity, whereas tight junctions remained morphologically intact in Ect2 and centralspindlin knockdown cells. This contrasts with the impact of p114 RhoGEF, which is recruited to tight junctions through an association with cingulin[44] and whose knockdown perturbed tight junctions but not cadherin-based adhesive junctions. This suggests that different GEFs may control different pools of Rho to support different junctions within the apical junctional complex and elsewhere in the contact zone between cells. Such a conclusion is consistent with the general paradigm that the action of specific GEFs may allow the common Rho signal to be utilized for different functional outcomes[1,40]. Further, while α-catenin was necessary to localise centralspindlin and Ect2 to the zonula adherens, it is noteworthy that α-catenin also distributes with E-cadherin more extensively outside the zonula adherens itself. Thus centralspindlin is unlikely to associate constitutively with α-catenin. Instead, other factors must collaborate to confer specificity for this interaction upon the pool of α-catenin associated with the zonula adherens itself.

Finally, our experiments also identify a role for dynamic microtubules to affect Rho signaling at the zonula adherens, apparently by influencing the capacity of the junctional cortex to bind Ect2. Thus, turnover analysis suggested that blocking dynamic microtubules might reduce junctional binding sites for Ect2 and, indeed, nocodazole treatment reduced junctional centralspindlin and its biochemical interaction with α-catenin, without affecting the α-catenin-cadherin interaction (not shown). Thus dynamic microtubules appear to regulate the interaction between centralspindlin and α-catenin. The detailed mechanism responsible for this effect remains to be clarified. During cytokinesis it has been proposed that centralspindlin mediates the microtubule-dependent delivery of Ect2 to the cytokinetic furrows[45]. Cell-cell junctions are regions that interact with and regulate microtubules[15,46,47], including a subpopulation that extend with their dynamic plus-ends directed towards the cortex of the junctions themselves[18]. Such dynamic microtubules could facilitate the delivery of centralspindlin by microtubule-dependent transport[48] or by serving as diffusional traps[47] that locally concentrate centralspindlin at the cortex. However, to date we have been unable to demonstrate microtubule-dependent transport of centralspindlin or Ect2 (not shown). Alternatively, dynamic microtubules might affect the binding of centralspindlin to α-catenin indirectly, by influencing cortical signaling[49]. These may include post-translational modifications, such protein phosphorylation, which influences Ect2 activation and its interaction with centralspindlin during cytokinesis[50]. Whether some of these pathways are also reused at the zonula adherens will be an important issue for future research.

Supplementary Material

Refer to Web version on PubMed Central for supplementary material.

Acknowledgments

We thank our laboratory colleagues for their support and advice, all our colleagues who provided generous gifts of reagents, and Rob Saint who first suggested we think about Ect2. This work was funded by the Human Frontiers Science Program, the National Health and Medical Research Council of Australia, Australian Research Council, and the Oncology Children's Foundation. Confocal microscopy was performed at the IMB/ACRF Cancer Biology Imaging Facility, established with the generous support of the Australian Cancer Research Foundation.

References

1. Jaffe AB, Hall A. Rho GTPases: biochemistry and biology. Annu Rev Cell Dev Biol. 2005; 21:247–269. doi:10.1146/annurev.cellbio.21.020604.150721. [PubMed: 16212495]
2. Bos JL, Rehmann H, Wittinghofer A. GEFs and GAPs: critical elements in the control of small G proteins. Cell. 2007; 129:865–877. doi:S0092-8674(07)00655-1 [pii] 10.1016/j.cell.2007.05.018. [PubMed: 17540168]
3. Miller AL, Bement WM. Regulation of cytokinesis by Rho GTPase flux. Nat Cell Biol. 2009; 11:71–77. doi:ncb1814 [pii] 10.1038/ncb1814. [PubMed: 19060892]
4. Pertz O, Hodgson L, Klemke RL, Hahn KM. Spatiotemporal dynamics of RhoA activity in migrating cells. Nature. 2006; 440:1069–1072. [PubMed: 16547516]
5. Yonemura S, Hirao-Minakuchi K, Nishimura Y. Rho localization in cells and tissues. Exp Cell Res. 2004; 295:300–314. doi:10.1016/j.yexcr.2004.01.005 S0014482704000138 [pii]. [PubMed: 15093731]
6. Yoshizaki H, et al. Activity of Rho-family GTPases during cell division as visualized with FRET-based probes. The Journal of cell biology. 2003; 162:223–232. [PubMed: 12860967]
7. Yamada S, Nelson WJ. Localized zones of Rho and Rac activities drive initiation and expansion of epithelial cell-cell adhesion. The Journal of cell biology. 2007; 178:517–527. doi:jcb.200701058 [pii] 10.1083/jcb.200701058. [PubMed: 17646397]

8. Bement WM, Miller AL, von Dassow G. Rho GTPase activity zones and transient contractile arrays. Bioessays. 2006; 28:983–993. [PubMed: 16998826]
9. Yuce O, Piekny A, Glotzer M. An ECT2-centralspindlin complex regulates the localization and function of RhoA. The Journal of cell biology. 2005; 170:571–582. doi:jcb.200501097 [pii] 10.1083/jcb.200501097. [PubMed: 16103226]
10. Magie CR, Pinto-Santini D, Parkhurst SM. Rho1 interacts with p120ctn and alpha-catenin, and regulates cadherin-based adherens junction components in Drosophila. Development. 2002; 129:3771–3782. [PubMed: 12135916]
11. Takaishi K, Sasaki T, Kotani H, Nishioka H, Takai Y. Regulation of cell-cell adhesion by Rac and Rho small G proteins in MDCK cells. J. Cell Biol. 1997; 139:1047–1059. [PubMed: 9362522]
12. Braga VMM, Machesky LM, Hall A, Hotchin NA. The small GPTases rho and rac are required for the formation of cadherin-dependent cell-cell contacts. J. Cell Biol. 1997; 137:1421–1431. [PubMed: 9182672]
13. Smutny M, et al. Myosin II isoforms identify distinct functional modules that support integrity of the epithelial zonula adherens. Nat Cell Biol. 2010; 12:696–702. doi:ncb2072 [pii] 10.1038/ncb2072. [PubMed: 20543839]
14. Carramusa L, Ballestrem C, Zilberman Y, Bershadsky AD. Mammalian diaphanous-related formin Dia1 controls the organization of E-cadherin-mediated cell-cell junctions. Journal of cell science. 2007; 120:3870–3882. doi:jcs.014365 [pii] 10.1242/jcs.014365. [PubMed: 17940061]
15. Meng W, Mushika Y, Ichii T, Takeichi M. Anchorage of microtubule minus ends to adherens junctions regulates epithelial cell-cell contacts. Cell. 2008; 135:948–959. [PubMed: 19041755]
16. Kametani Y, Takeichi M. Basal-to-apical cadherin flow at cell junctions. Nat Cell Biol. 2007; 9:92–98. [PubMed: 17159998]
17. Wolfe BA, Glotzer M. Single cells (put a ring on it). Genes Dev. 2009; 23:896–901. doi:23/8/896 [pii] 10.1101/gad.1801209. [PubMed: 19390083]
18. Stehbens SJ, et al. Dynamic microtubules regulate the local concentration of E-cadherin at cell-cell contacts. Journal of cell science. 2006; 119:1801–1811. [PubMed: 16608875]
19. Jordan MA, Wilson L. Use of drugs to study role of microtubule assembly dynamics in living cells. Methods Enzymol. 1998; 298:252–276. [PubMed: 9751887]
20. Perez F, Diamantopoulos GS, Stalder R, Kreis TE. CLIP-170 highlights growing microtubule ends in vivo. Cell. 1999; 96:517–527. [PubMed: 10052454]
21. Shewan AM, et al. Myosin 2 Is a Key Rho Kinase Target Necessary for the Local Concentration of E-Cadherin at Cell-Cell Contacts. Mol Biol Cell. 2005; 16:4531–4532. [PubMed: 16030252]
22. Komarova Y, et al. Mammalian end binding proteins control persistent microtubule growth. The Journal of cell biology. 2009; 184:691–706. doi:jcb.200807179 [pii] 10.1083/jcb.200807179. [PubMed: 19255245]
23. Komarova Y, et al. EB1 and EB3 control CLIP dissociation from the ends of growing microtubules. Mol Biol Cell. 2005; 16:5334–5345. doi:E05-07-0614 [pii] 10.1091/mbc.E05-07-0614. [PubMed: 16148041]
24. Tatsumoto T, Xie X, Blumenthal R, Okamoto I, Miki T. Human ECT2 is an exchange factor for Rho GTPases, phosphorylated in G2/M phases, and involved in cytokinesis. The Journal of cell biology. 1999; 147:921–928. [PubMed: 10579713]
25. Somers WG, Saint R. A RhoGEF and Rho family GTPase-activating protein complex link the contractile ring to cortical microtubules at the onset of cytokinesis. Develop Cell. 2003; 4:29–39. [PubMed: 12530961]
26. Liu XF, Ishida H, Raziuddin R, Miki T. Nucleotide exchange factor ECT2 interacts with the polarity protein complex Par6/Par3/protein kinase Czeta (PKCzeta) and regulates PKCzeta activity. Molecular and cellular biology. 2004; 24:6665–6675. [PubMed: 15254234]
27. Sawyer JM, et al. Apical constriction: a cell shape change that can drive morphogenesis. Dev Biol. 2010; 341:5–19. doi:S0012-1606(09)01178-6 [pii] 10.1016/j.ydbio.2009.09.009. [PubMed: 19751720]
28. Miyake Y, et al. Actomyosin tension is required for correct recruitment of adherens junction components and zonula occludens formation. Exp Cell Res. 2006; 312:1637–1650. [PubMed: 16519885]

29. Smutny M, et al. Multicomponent analysis of junctional movements regulated by myosin II isoforms at the epithelial zonula adherens. PLoS One. 2011; 6:e22458. [PubMed: 21799860]
30. Kasza KE, Zallen JA. Dynamics and regulation of contractile actin–myosin networks in morphogenesis. Current opinion in cell biology. 2011; 23:30–38. doi:S0955-0674(10)00185-7 [pii] 10.1016/j.ceb.2010.10.014. [PubMed: 21130639]
31. Monier B, Pelissier-Monier A, Brand AH, Sanson B. An actomyosin-based barrier inhibits cell mixing at compartmental boundaries in Drosophila embryos. Nat Cell Biol. 2009; 12:60–65. doi:ncb2005 [pii] 10.1038/ncb2005. [PubMed: 19966783]
32. Fernandez-Gonzalez R, Simoes Sde M, Roper JC, Eaton S, Zallen JA. Myosin II dynamics are regulated by tension in intercalating cells. Dev Cell. 2009; 17:736–743. doi:S1534-5807(09)00385-2 [pii] 10.1016/j.devcel.2009.09.003. [PubMed: 19879198]
33. Mishima M, Kaitna S, Glotzer M. Central spindle assembly and cytokinesis require a kinesin-like protein/RhoGAP complex with microtubule bundling activity. Dev Cell. 2002; 2:41–54. doi:S1534580701001101 [pii]. [PubMed: 11782313]
34. Hirose K, Kawashima T, Iwamoto I, Nosaka T, Kitamura T. MgcRacGAP is involved in cytokinesis through associating with mitotic spindle and midbody. J Biol Chem. 2001; 276:5821–5828. doi:10.1074/jbc.M007252200 M007252200 [pii]. [PubMed: 11085985]
35. Mikawa M, Su L, Parsons SJ. Opposing roles of p190RhoGAP and Ect2 RhoGEF in regulating cytokinesis. Cell Cycle. 2008; 7:2003–2012. [PubMed: 18642445]
36. Wildenberg GA, et al. p120-catenin and p190RhoGAP regulate cell-cell adhesion by coordinating antagonism between Rac and Rho. Cell. 2006; 127:1027–1039. doi:S0092-8674(06)01407-3 [pii] 10.1016/j.cell.2006.09.046. [PubMed: 17129786]
37. Noren NK, Arthur WT, Burridge K. Cadherin Engagement Inhibits RhoA via p190RhoGAP. J Biol Chem. 2003; 278:13615–13618. [PubMed: 12606561]
38. Manchinelly SA, et al. Mitotic down-regulation of p190RhoGAP is required for the successful completion of cytokinesis. J Biol Chem. 2010; 285:26923–26932. doi:M110.103804 [pii] 10.1074/jbc.M110.103804. [PubMed: 20534586]
39. Su L, Pertz O, Mikawa M, Hahn K, Parsons SJ. p190RhoGAP negatively regulates Rho activity at the cleavage furrow of mitotic cells. Exp Cell Res. 2009; 315:1347–1359. doi:S0014-4827(09)00075-5 [pii] 10.1016/j.yexcr.2009.02.014. [PubMed: 19254711]
40. Bustos RI, Forget MA, Settleman JE, Hansen SH. Coordination of Rho and Rac GTPase function via p190B RhoGAP. Curr Biol. 2008; 18:1606–1611. doi:S0960-9822(08)01243-8 [pii] 10.1016/j.cub.2008.09.019. [PubMed: 18948007]
41. Burbelo PD, et al. p190-B, a new member of the Rho GAP family, and Rho are induced to cluster after integrin cross-linking. J Biol Chem. 1995; 270:30919–30926. [PubMed: 8537347]
42. Scott JA, Yap AS. Cinderella no longer: alpha-catenin steps out of cadherin's shadow. Journal of cell science. 2006; 119:4599–4605. [PubMed: 17093264]
43. Lien WH, Klezovitch O, Vasioukhin V. Cadherin-catenin proteins in vertebrate development. Current opinion in cell biology. 2006; 18:499–506. [PubMed: 16859905]
44. Terry SJ, et al. Spatially restricted activation of RhoA signalling at epithelial junctions by p114RhoGEF drives junction formation and morphogenesis. Nat Cell Biol. 2011; 13:159–166. doi:ncb2156 [pii] 10.1038/ncb2156. [PubMed: 21258369]
45. Saint R, Somers WG. Animal cell division: a fellowship of the double ring? Journal of cell science. 2003; 116:4277–4281. [PubMed: 14514883]
46. Bellett G, et al. Microtubule plus-end and minus-end capture at adherens junctions is involved in the assembly of apico-basal arrays in polarised epithelial cells. Cell Motil Cytoskeleton. 2009; 66:893–908. doi:10.1002/cm.20393. [PubMed: 19479825]
47. Stehbens SJ, Akhmanova A, Yap AS. Microtubules and cadherins: a neglected partnership. Front Biosci. 2009; 14:3159–3167. doi:3442 [pii]. [PubMed: 19273264]
48. Akhmanova A, Stehbens SJ, Yap AS. Touch, grasp, deliver and control: functional cross-talk between microtubules and cell adhesions. Traffic. 2009; 10:268–274. doi:TRA869 [pii] 10.1111/j.1600-0854.2008.00869.x. [PubMed: 19175539]
49. Rodriguez OC, et al. Conserved microtubule-actin interactions in cell movement and morphogenesis. Nat Cell Biol. 2003; 5:599–609. [PubMed: 12833063]

50. Wolfe BA, Takaki T, Petronczki M, Glotzer M. Polo-like kinase 1 directs assembly of the HsCyk-4 RhoGAP/Ect2 RhoGEF complex to initiate cleavage furrow formation. PLoS Biol. 2009; 7:e1000110. doi:10.1371/journal.pbio.1000110. [PubMed: 19468300]

Europe PMC Funders Author Manuscripts

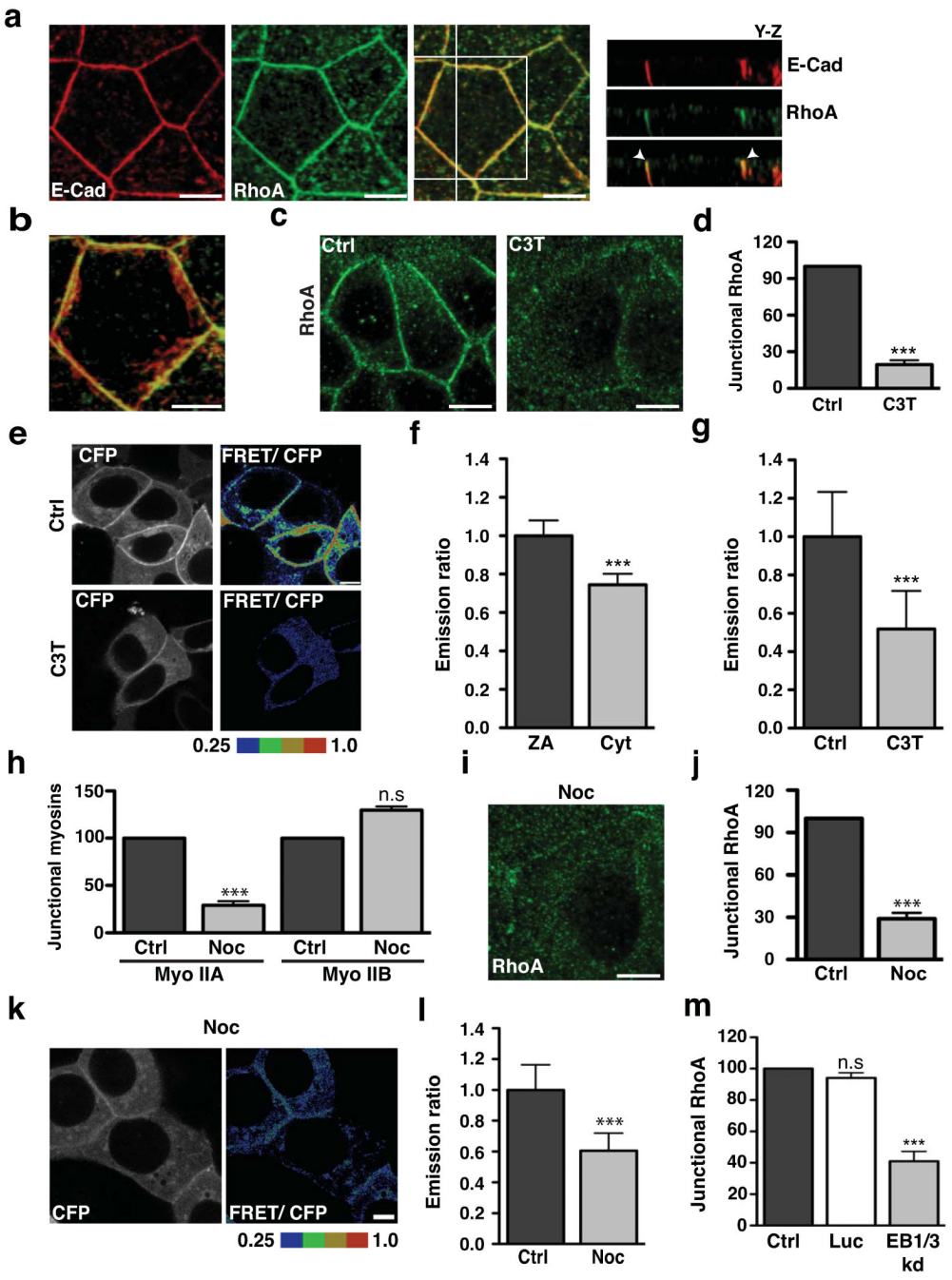

Figure 1. The zonula adherens is a microtubule-dependent Rho zone

(a-b) Apical junctions in TCA-fixed MCF-7 monolayers immunostained for E-Cadherin (E-Cad, red) and RhoA (green) imaged by confocal microscopy. The distribution of proteins along the *z*-axis of cells is represented in *y*-*z* views (taken at the vertical line) (a) and the magnification (b) shows colocalisation of E-cadherin with RhoA at the ZA in a maximum intensity projection. Arrowheads indicate accumulation of E-cadherin and RhoA at the ZA (a).

(c-d) Confluent MCF-7 cells treated with either C3 Transferase (C3T; 0.25 μg/ml) or glycerol (vehicle, Ctrl) for one hour and then fixed and stained for RhoA. Representative confocal images were taken from the apical junctions (c) and fluorescence intensity at cell

junctions was quantitated by linescan analysis (d). Data represent control-normalized means ± S.E.M. of data pooled from three individual experiments (n=30), ***P<0.0001; Student's t-test.

(e-g) Confluent MCF-7 cells expressing a RhoA-FRET biosensor were treated as in c-d and imaged live using confocal microscopy. Images were acquired in the CFP and FRET channels and representative images (CFP and ratio of FRET/CFP) are shown (e). Average emission ratios were determined at the apical junctions and the cytoplasm of control cells as described in methods (f). To determine the effect of C3T on junctional RhoA activity, average emission ratios were quantitated at the apical junctions (g). Data represent junctional-(f) or control-normalized (g) means ± S.E.M. of data pooled from three individual experiments (n=26), ***P<0.0001; Student's t-test.

(h) Confluent MCF-7 cells were treated with DMSO (Ctrl) or Nocodazole (100nM, 3h) and fluorescence intensity of myosin (Myo) IIA and IIB at cell junctions was quantitated by linescan analysis. Data represent control-normalized means ± S.E.M. of data pooled from three individual experiments (n=25), ***P<0.001; Student's t-test.

(i-j) Control and Nocodazole-treated cells were fixed and stained for RhoA. Representative apical confocal images were taken (i) and junctional RhoA was quantitated by linescan analysis (j). Data represent control-normalized means ± S.E.M. of data pooled from three individual experiments (n=30), ***P<0.001; Student's t-test.

(k-l) Confluent MCF-7 cells expressing a RhoA-FRET Biosensor were treated with Nocodazole (as in h) and imaged live using confocal microscopy. CFP and ratio of FRET/CFP representative images are shown (k) and average emission ratios were quantified at the apical junctions (l). Data represent control-normalized means ± S.E.M. of data pooled from three individual experiments (n=40), ***P<0.001; Student's t-test.

(m) MCF-7 cells were transfected with pECFP-C1 (Ctrl) or with pSUPER constructs containing shRNAs against Luciferase (Luc) or EB1 + EB3 (EB1/3 kd) and fixed after 48 hours. Junctional RhoA in CFP-positive cells was quantitated by linescan analysis. Data represents control-normalized means ± S.E.M. of data pooled from three individual experiments (n=15), *** P<0.001; One way Anova, Dunnett's post hoc test.

Scale bars: a,c,i 10μm; b,e,l 5 μm.

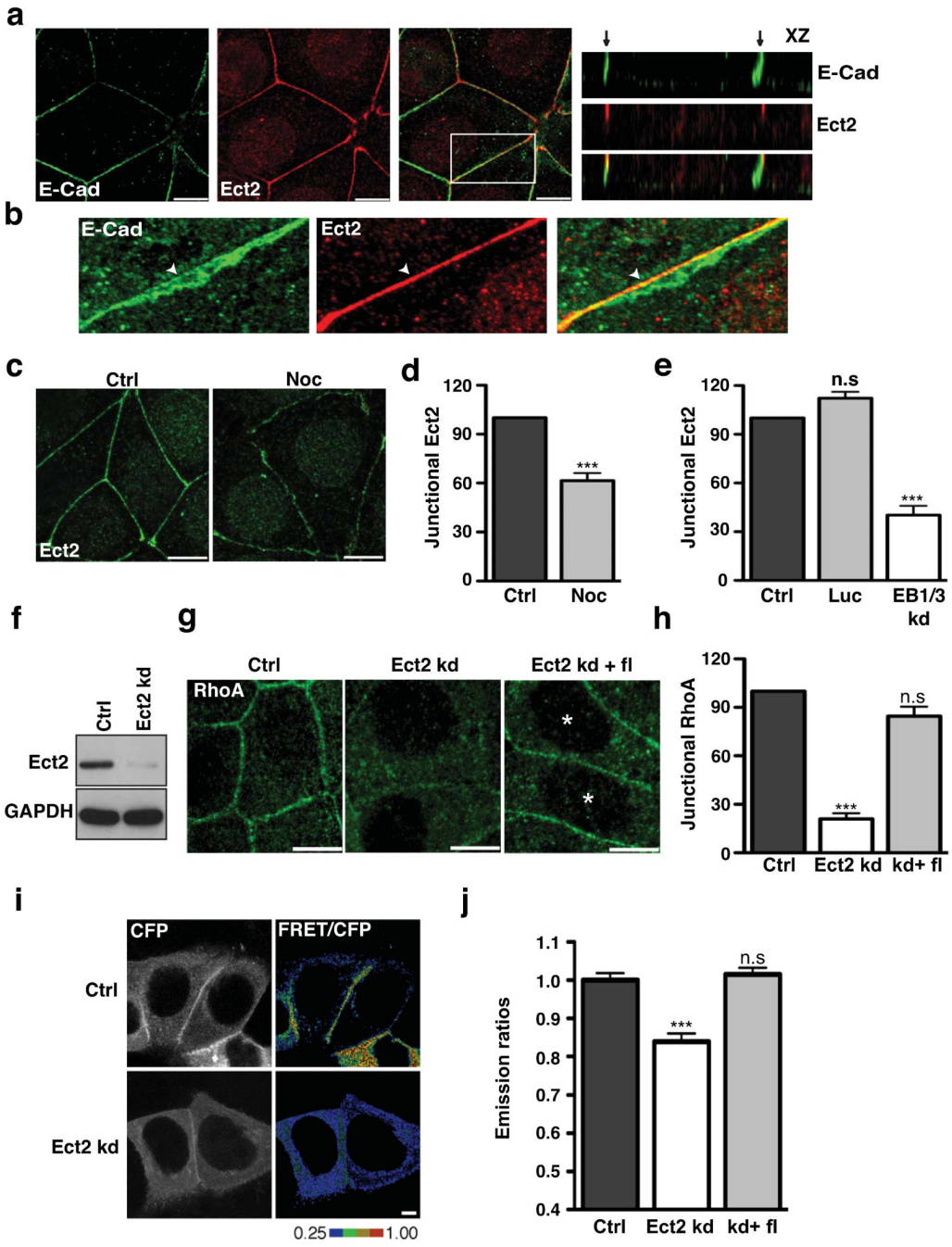

Figure 2. Ect2 is a junctional RhoA GEF

(a-b) Confluent MCF-7 cells were fixed and immunostained for E-Cadherin (E-Cad, green) and Ect2 (red). Representative confocal images at the zonula adherens (a) and *x-z* views illustrating the distribution of proteins along the *z* axis of cells. Arrows indicate the apical tips of cell–cell contacts. (b) Magnification shows colocalisation of E-cadherin with Ect2 at the ZA in a maximum intensity projection. Arrowheads indicate accumulation of E-cadherin and Ect2 at the ZA.

(c-d) Confluent MCF-7 cells treated with or without Nocodazole (Noc and Ctrl) were fixed and stained for Ect2. Representative confocal images were taken from the apical junctions

Europe PMC Funders Author Manuscripts

(c) and junctional Ect2 was quantitated by linescan analysis (d). Data represent control-normalized means ± S.E.M. of data pooled from three individual experiments (n=30), ***P<0.001; Student's t-test.
(e) MCF-7 cells were transfected with pECFP-C1 (Ctrl) or with pSUPER constructs containing shRNAs against Luciferase (Luc) or EB1 + EB3 (EB1/3 kd). Junctional Ect2 in CFP-positive cells was quantified by linescan analysis; data represent control-normalized means ± S.E.M. of data pooled from three individual experiments (n=15), ***P<0.001; One way Anova, Dunnett's post hoc test.
(f) Lysates from MCF-7 cells infected with lentivirus bearing an empty vector control (Ctrl) or an shRNA-directed against Ect2 (Ect2 kd) were immunoblotted for Ect2 and GAPDH (loading control).
(g-h) Rho immunofluorescence in control (Ctrl), Ect2 knockdown (Ect2 kd) cells, and Ect2 kd cells transiently expressing shRNA-resistant EGFP-Ect2 (Ect2kd + fl). Representative confocal images were taken from the apical junctions of cells (g) and junctional RhoA was quantitated using linescan analysis (h). Asterisks mark cells transfected with EGFP-Ect2. Data represent control-normalized means ± S.E.M. of data pooled from three individual experiments (n=15), ***P<0.001; One way Anova, Dunnett's post hoc test.
(i-j) Control (Ctrl), Ect2 knockdown (Ect2 kd) and Ect2 kd cells expressing RNAi-resistant Ect2 (kd+fl) cells were transfected with a RhoA-FRET Biosensor and imaged live using confocal microscopy. Representative images of CFP and ratio of FRET/CFP are shown (i) and average emission ratios were quantified at the apical junctions (j). Data represent control-normalized means ± S.E.M. of data pooled from three individual experiments (n=43), ***P<0.001; Student's t-test.
Scale bars: a,c,g 10 μm; i 5 μm.

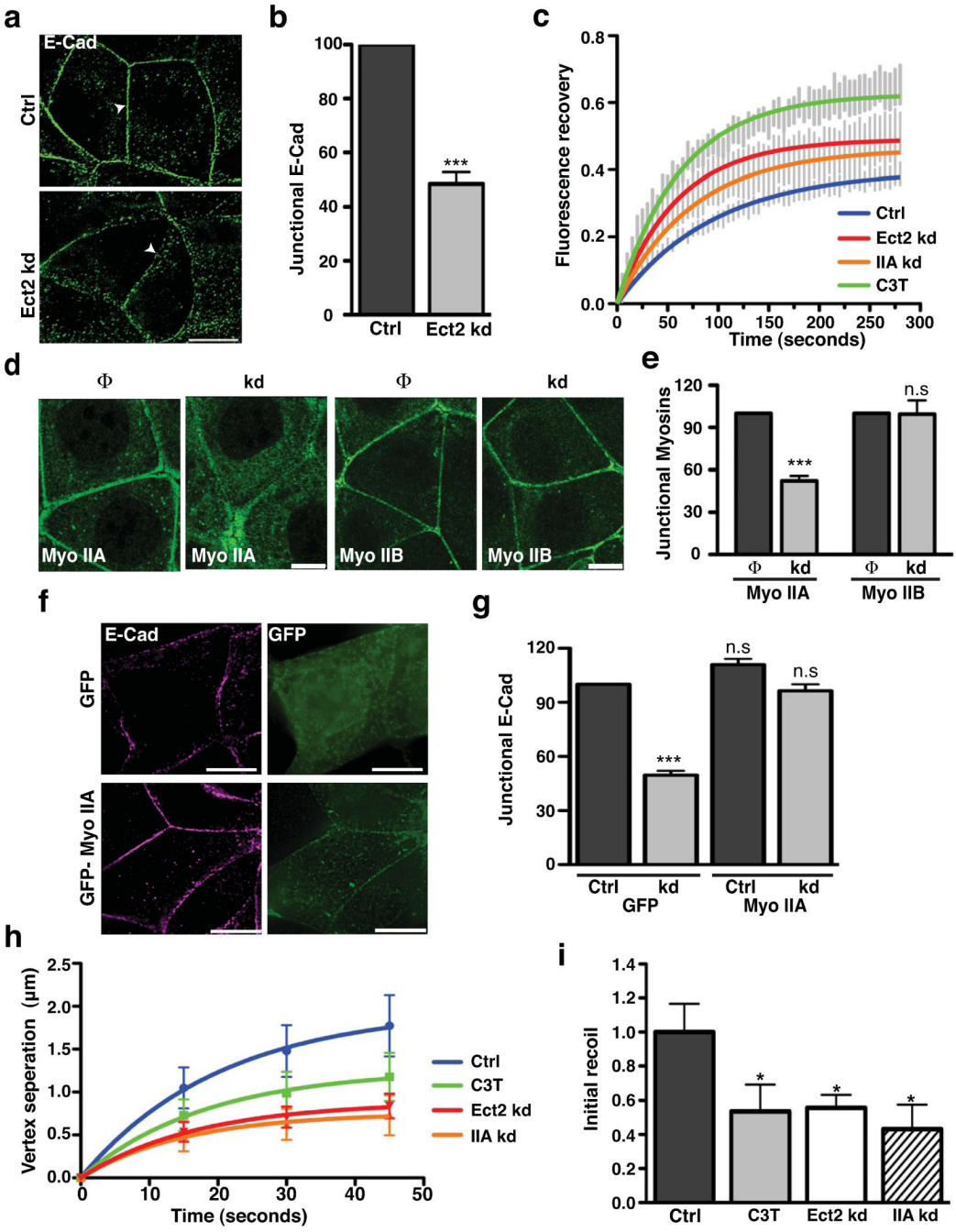

Figure 3. Ect2 is necessary for zonula adherens integrity and junctional tension

(a-b) E-cadherin (E-Cad) immunostaining in Control (Ctrl) and Ect2 knockdown (Ect2 kd) cells imaged by wide-field deconvolution microscopy (a; arrowheads indicate apical junctional region). Peak junctional fluorescence intensity (b) was measured by line scan analysis. Data represent control-normalized means ± S.E.M. of data pooled from three individual experiments (n=25; ***P<0.001; Student's t-test).

(c) Fluorescence recovery after photobleaching was performed for E-cadherin-GFP (expressed in MCF-7 cells depleted of endogenous E-cadherin by RNAi; Ctrl) or also treated with C3T (C3T) or RNAi to Ect2 (Ect2 kd) or myosin IIA (IIA kd). Vertical lines represent means ± S.E.M. and solid lines are best-fit single exponential curves.

(d-e) Myosin IIA or myosin IIB at cell junctions were analysed in control (Φ) and Ect2 knockdown (kd) cells by immunofluorescence (f) and quantitated by linescan analysis (g). Data represent control-normalized means ± S.E.M. of data pooled from three individual experiments (n=20-25),***P<0.001; Student's t-test.
(f,g) Control (Ctrl) and Ect2 knockdown (kd) cells transfected with either pEGFP-C1 (GFP) or EGFP-MyoIIA (GFP-Myo IIA) were fixed and stained for E-cadherin (E-Cad,magenta) and GFP (green). Representative epi-illumination images were taken from the apical junctions of Ect2 knockdown cells (f). Junctional E-cadherin fluorescence intensity (g) was analysed by line scan analysis. Data represent control-normalized means ± S.E.M. of data pooled from three individual experiments (n=10-25; ***P<0.001; One way Anova, Dunnett's post hoc test.
(h,i) Junctional tension was measured by laser nanoscissors in control (Ctrl) MCF-7 cells and cells treated with C3T (C3T) or RNAi to Ect2 (Ect2 kd) or myosin IIA (IIA kd). Vertex displacement (h) and initial recoil (i) are shown (n=9-14; *P<0.05; t-test).
Scale bars 10 μm.

Europe PMC Funders Author Manuscripts

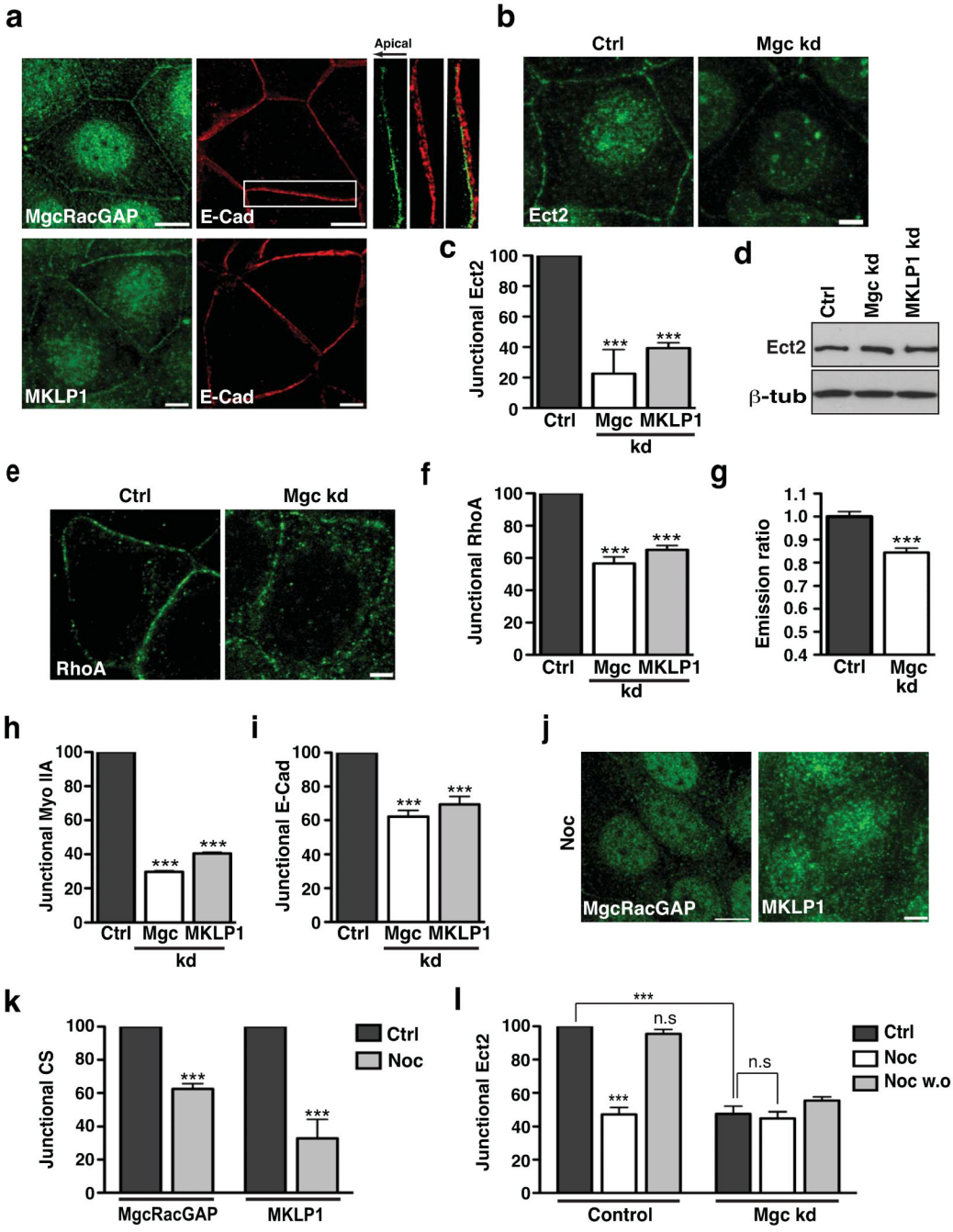

Figure 4. Centralspindlin regulates junctional Ect2-Rho signalling

(a) Confluent MCF-7 cells were immunostained for E-Cadherin (E-Cad, red) and either MgcRacGAP (MgcRacGAP) or MKLP1 (green). Representative apical confocal images are shown. Magnification shows colocalisation of E-cadherin with MgcRacGAP at the ZA in a maximum intensity projection (direction of the arrow indicates basal to apical).

(b-d) MCF-7 cells were transfected with siRNAs against MgcRacGAP (Mgc kd), MKLP1 (MKLP1 kd) or with scrambled siRNA (Ctrl). Cells were fixed after 48 hours and stained for Ect2. Representative confocal images were taken (b) and junctional Ect2 was quantified by linescan analysis (c). Data represent control-normalized means ± S.E.M. of data pooled from three individual experiments (n=25; *** P<0.001; One way Anova, Dunnett's post hoc

test). (d) Lysates from control, MgcRacGAP knockdown and MKLP1 knockdown cells were immunoblotted for Ect2 and β tubulin (β tub).
(e-i) Control (Ctrl), MgcRacGAP knockdown (Mgc kd) and MKLP1 knockdown (MKLP1 kd) cells were fixed and stained for RhoA, myosin IIA or E-cadherin and Rho-GTP was measured by FRET in Ctrl and Mgc kd cells. Representative confocal images of RhoA staining at the apical junctions are shown (e) with quantified junctional RhoA (f), Rho-GTP (g), Myo IIA (h) and E-Cad (i). Data represent control-normalized means ± S.E.M. of data pooled from three individual experiments for RhoA (f), Myo IIA(h) and E-Cad (i) (n=20-25; ***P<0.001; One way Anova, Dunnett's post hoc test). For Rho-GTP (g), data represent means ± S.E.M. of data pooled from three individual experiments (n = 59-85, ***P<0.001; Student's t-test).
(j-k) Confluent MCF-7 cells treated with Nocodazole (Noc) were fixed and stained for MgcRacGAP or MKLP1. Representative confocal images were taken (j) and fluorescence intensity at junctions was quantitated by linescan analysis (k). Data represent control-normalized mean ± S.E.M. of data pooled from three individual experiments (n=30), ***P<0.001; Student's t-test.
(l) MCF-7 cells were transfected with siRNAs against MgcRacGAP (Mgc kd) or scrambled (control) siRNA. 48 hours post transfection, the cells were incubated for 3 hours with 100nM Nocodazole (Noc) or DMSO (Ctrl) after which Nocodazole was washed out and cells allowed to recover for 1 hour (Noc w.o). Cells were then fixed and stained for Ect2 and junctional Ect2 was quantified using linescan analysis. Data represent control-normalized means ± S.E.M. of data pooled from three individual experiments (n=15; ***P<0.001; One way Anova, Bonferroni post hoc test, to compare across all data sets).
Scale bars a,j: MgcRacGAP 10μm, MKLP1 5μm; b:10μm, e: 5μm.

Europe PMC Funders Author Manuscripts

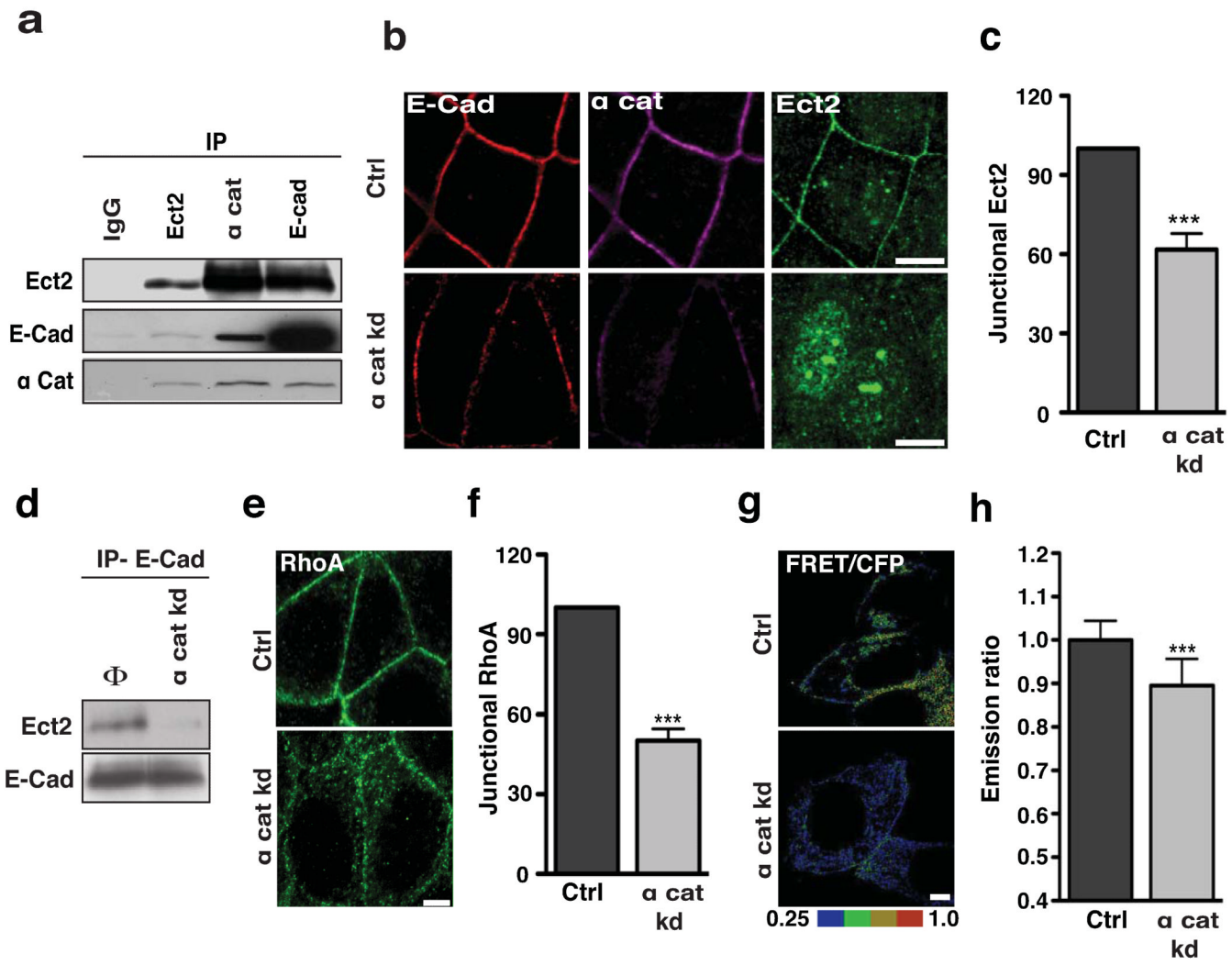

Figure 5. α-catenin mediates the junctional retention of Ect2

(a) Immunoprecipitates of Ect2, E-Cadherin (E-Cad) or α-catenin (α cat) were immunoblotted for Ect2, E-Cadherin and α-catenin. Rabbit IgG (IgG) was used as a negative control for the immunoprecipitation.

(b-c) MCF-7 cells transfected with SMARTpool siRNA against α-catenin (α cat kd) or non-targeting siRNA pools (Ctrl) were fixed and stained for E-Cadherin (red), α cat (magenta) and Ect2 (green). Representative apical confocal images were taken (b) and accumulation of Ect2 was quantitated by linescan analysis (c). Data represent control-normalized means ± S.E.M. of data pooled from three individual experiments (n=25; ***P<0.001; Student's t-test).

(d) Immunoprecipitates of E-Cadherin (IP-E-Cad) from MCF-7 cells transfected with SMARTpool siRNA against α- catenin (α cat kd) or non-targeting siRNA pools (Φ) were immunoblotted for Ect2 and E-cadherin (E-Cad).

(e-f) Control (Ctrl) and α-catenin knockdown (α cat kd) cells were fixed and stained for RhoA. Representative apical confocal images were taken (e) and accumulation of RhoA was quantitated by linescan analysis (f). Data represent control-normalized means ± S.E.M. of data pooled from three individual experiments (n=25; ***P<0.001; Student's t-test).

(g-h) MCF-7 cells transfected simultaneously with a Rho-FRET Biosensor and a SMARTpool siRNA against α-catenin (α cat kd) or non-targeting siRNA pools (Ctrl) were

imaged by live-cell confocal microscopy after 36 h. Representative images of the ratio of FRET/CFP are shown (g) and average emission ratios were quantitated at the apical junctions (h). Data represent control-normalized means ± S.E.M. of data pooled from three individual experiments (n=46-52).
Scale bars: b 10 μm, e,g 5 μm.

Europe PMC Funders Author Manuscripts

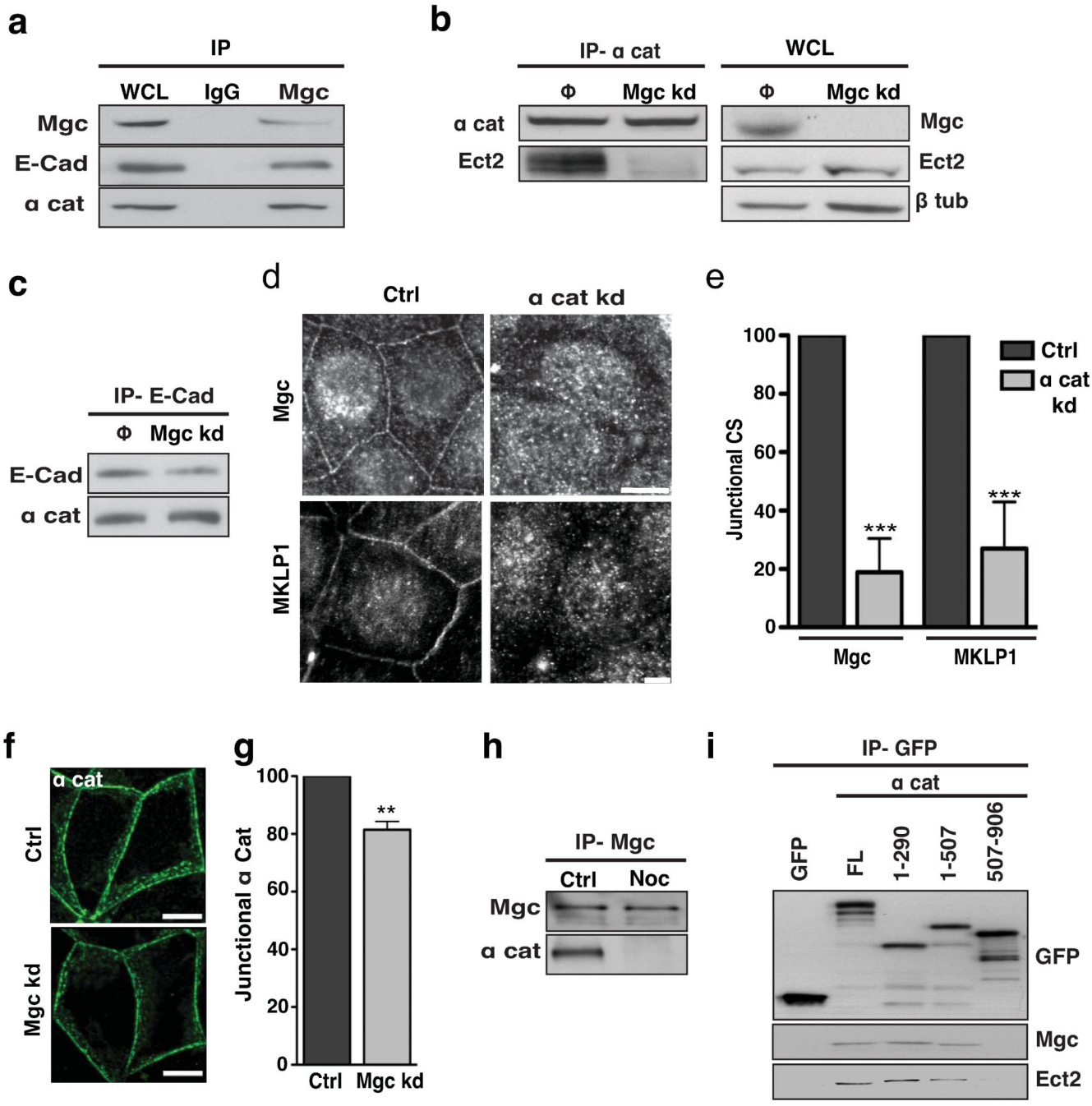

Figure 6. α-catenin mediates the junctional retention of Centralspindlin

(a) Whole cell lysates from MCF-7 cells (WCL) and Mgc RacGAP immunoprecipitates were immunoblotted for MgcRacGAP (Mgc), E-Cadherin (E-Cad) and α-catenin (α cat). Rabbit IgG (IgG) was used as a negative control for the immunoprecipitation.

(b) α-catenin immunoprecipitates from control (Φ) and MgcRacGAP kd cells (Mgc kd) were immunoblotted for α-catenin (α-cat) and Ect2. Whole cell lysates (WCL) from control and MgcRacGAP kd cells were immunoblotted for MgcRacGAP (Mgc), Ect2 and β-tubulin.

(c) E-cadherin immunoprecipitates from Control (Φ) and MgcRacGAP kd (Mgc kd) cells immunoblotted for E-Cadherin and α-catenin.

(d-e) MCF-7 cells were transfected with SMARTpool siRNA against α-catenin (α cat kd) or non-targeting siRNA pools (Ctrl) and 36 h later fixed and stained for MgcRacGAP (Mgc) or MKLP1. Representative apical confocal images were taken (d) and accumulation of MgcRacGAP and MKLP1 (CS) was quantitated by linescan analysis (e). Data represent control-normalized means ± S.E.M. of data pooled from three individual experiments (n=25; ***P<0.001; Student's t-test).
(f-g) MCF-7 cells were transfected with siRNAs against MgcRacGAP (Mgc kd) or scrambled (Ctrl) siRNA. Cells were fixed after 48 hours and stained for α-catenin (α cat, green). Representative apical confocal images were taken (f) and accumulation of α- catenin was quantitated by linescan analysis (g). Data represent control-normalized means ± S.E.M. of data pooled from three individual experiments (n=25; ** *P*<0.005;Student's t-test).
(h) MgcRacGAP (Mgc) immunoprecipitates from control (Ctrl) and nocodazole (Noc)-treated MCF-7 cells were immunoblotted for MgcRacGAP and α-catenin.
(i) GFP-tagged full-length (FL) α-catenin or truncation mutants were transiently expressed in HEK293 cells, isolated by GFP trap and then immunoblotted for GFP, MgcRacGAP (Mgc) or Ect2. The mutants are illustrated in Supplementary Fig S5d.
Scale bars. d:RacGAP1,10μm, MKLP1 60μm, f: 10μm.

Europe PMC Funders Author Manuscripts

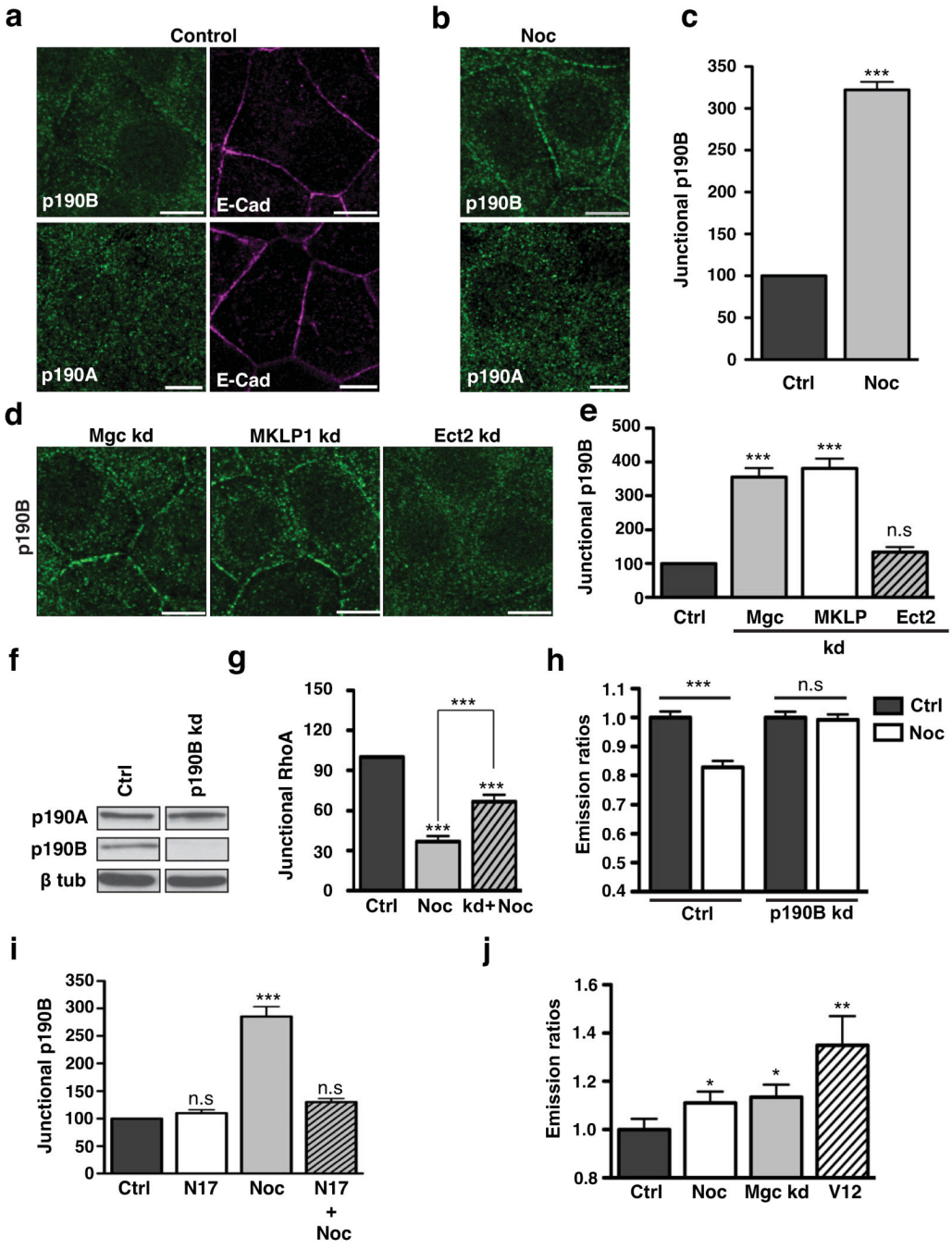

Figure 7. Centralspindlin inhibits the junctional recruitment of p190B RhoGAP

(a-c) Control (a) and nocodazole (100 nM, 3h)-treated MCF-7 cells (b) were immunostained for E-Cadherin (E-Cad, magenta) and either p190A RhoGAP or p190B RhoGAP (green). Representative confocal images were taken from the apical junctions of the cells. Junctional p190B was quantitated in control and Nocodazole treated cells by linescan analysis (c). Data represent control-normalized means ± S.E.M. of data pooled from three individual experiments (n=60; ***P<0.001; Student's t-test).

(d-e) MCF-7 cells were transfected with siRNAs against MgcRacGAP (Mgc kd), MKLP1 (MKLP kd) or scrambled (ctrl) siRNA, or infected with lentivirus bearing an shRNA directed against Ect2 (Ect2 kd cells). Cells were fixed after 48 hours, stained for p190B

RhoGAP and imaged at the apical junctions by confocal microscopy (d). Junctional p190B RhoGAP was quantified by linescan analysis (e). Data represent control-normalized means ± S.E.M. of data pooled from three individual experiments (n=25; ***P<0.001;One way Anova, Dunnett's post hoc test).

(f) MCF7 cells were transfected with non-targeting siRNA pools (Ctrl) or SMARTpool siRNA against p190B RhoGAP (p190B kd) for 48 hours. Whole cell lysates from control (Ctrl) and p190B RhoGAP kd cells were immunoblotted for p190A RhoGAP, p190B RhoGAP or β-tubulin.

(g,h) Junctional Rho or Rho-GTP in control and p190B RhoGAP kd cells incubated with or without nocodazole (100 nM, 3h). Endogenous junctional Rho (g) was quantified by linescan analysis. Data represent control-normalized means ± S.E.M. of data pooled from three individual experiments (n=25; ***P<0.001;One way Anova, Bonferroni post hoc test, to compare across all data sets). Rho-GTP (h) was measured using a transiently-expressed Rho FRET biosensor. Data represent control-normalized means ± S.E.M. of data pooled from three individual experiments (n=50-86; ***P<0.001; Students t-test.

(i) MCF-7 cells were transfected with EGFP pcDNA3.1 (Ctrl) or GFP-N17 Rac1 DN-pcDNA3.1 (N17), then treated with nocodazole (100 nM, 3 h). Junctional p190B RhoGAP was quantitated by linescan analysis. Data represent control-normalized means ± S.E.M. of data pooled from three individual experiments (n=25; ***P<0.001;One way Anova, Dunnett's post hoc test).

(j) Junctional Rac-GTP was measured with a Raichu-Rac biosensor in control (Ctrl) cells or cells treated with nocodazole (100 nM, 3 hrs), MgcRacGAP siRNA (Mgc kd) or a transiently expressed constitutively-active Rac mutant (V12). Data represent means ± S.E.M. of data pooled from three individual experiments (n=30, *P<0.05; Student's t-test). Scale bars are 10μm.

Europe PMC Funders Author Manuscripts